Journal of Materiomics 8 (2022) 669–677

Contents lists available at ScienceDirect

Journal of Materiomics

journal homepage: www.journals.elsevier.com/journal-of-materiomics/

Research paper

Competition between axial anomaly and ferromagnetic ordering in $Bi_{2-x}Fe_xSe_{3-x}S_x$ topological insulator: A study of magnetic and magnetotransport properties

Rahul Singh [a], Shiv Kumar [b, 2], A. Jain [a, c, 2], Mahima Singh [d], Labanya Ghosh [d], A. Singh [d, 1], Soma Banik [e], A. Lakhani [f], S. Patil [d], E.F. Schwier [b], K. Shimada [b], S.M. Yusuf [a, c, **], Sandip Chatterjee [d, *]

[a] Solid State Physics Division, Bhabha Atomic Research Center, Trombay, Mumbai, 400085, India
[b] Hiroshima Synchrotron Radiation Center, Hiroshima, Japan
[c] Homi Bhabha National Institute, Anushaktinagar, Mumbai, 400094, India
[d] Department of Physics, Indian Institute of Technology (BHU), Varanasi, 221005, India
[e] Synchrotrons Utilization Section, Raja Ramanna Centre for Advanced Technology, Indore, 452013, India
[f] UGC-DAE Consortium for Scientific Research, Indore, Madhya Pradesh, 452017, India

ARTICLE INFO

Article history:
Received 4 August 2021
Received in revised form
5 November 2021
Accepted 11 November 2021
Available online 15 November 2021

Keywords:
Spintronics
Magnetoresistance
Magnetism
Topological insulators
RKKY interaction
ARPES study

ABSTRACT

The topological insulators $Bi_{2-x}Fe_xSe_{3-x}S_x$ have been investigated by the dc-magnetization, magneto-transport and angle resolved photoemission spectroscopy (ARPES) techniques. With doping of Fe and S, a negative giant magneto-resistance (MR) is observed for parallel electric and magnetic fields ($H||E$). The MR behavior at lower magnetic field can be explained with the semi-classical theory whereas the MR behavior at higher field has been attributed to the axial anomaly. Interestingly, the system reached to the quantum limit at low magnetic field (~ 4.5T). The magnetic ordering can be explained with the presence of both the RKKY (surface) and van-Vleck (bulk) interaction. The ARPES study reveals that a surface gap is suppressed when the magnetic ordering changes from ferromagnetic to anti-ferromagnetic ordering. The ARPES study and the appearance of quantum oscillations (SdH) in the resistivity pattern reveal that the topological surface property is preserved with the co-doping of Fe and S.

1. Introduction

The observation of negative magnetoresistance (MR) in topological semi-metals and topological insulators(TIs), when a magnetic field is applied parallel to an electric field (called longitudinal geometry), has recently attracted lots of attention [1–8]. For the topological semi-metals, the observed negative longitudinal MR has been ascribed to the presence of chiral anomaly, where the conservation of chiral current is violated due to the quantization [3,7,8]. In view of this, the observation of negative longitudinal MR in the epitaxial thin film of stoichiometric Bi_2Se_3 [9] canonical 3D topological insulator, where chirality is not well defined, has attracted a renewed interest [9–11]. The observed negative longitudinal MR was attributed to an axial symmetry and it was argued that the axial symmetry may give rise to far more generic phenomenon in a topological insulator [9]. In a recent study [12], a very small (<1 %) negative MR was reported for the S doped bulk Bi_2Se_3. The low negative MR (NMR) has also been reported in the $TlBi_{0.15}Sb_{0.85}Te_2$ system where at low temperature the resistivity is thermally activated [13]. Recently, it was theoretically proposed that the NMR is a generic property of semiconductors and metals,

* Corresponding author.
** Corresponding author. Solid State Physics Division, Bhabha Atomic Research Center, Trombay, Mumbai, 400085, India.
E-mail addresses: smyusuf@barc.gov.in (S.M. Yusuf), schatterji.app@iitbhu.ac.in (S. Chatterjee).
Peer review under responsibility of The Chinese Ceramic Society.
[1] Present Address: Department of CMP &MS, Tata Institute of Fundamental Research, Mumbai, 400005, India.
[2] Equally contributed.

https://doi.org/10.1016/j.jmat.2021.11.005

rather than limited to the topological semi-metals [14]. By using the semi-classical equations of motion, Dai *et al.* [15] recently ascribed the NMR of a TI to the Berry curvature induced anomalous velocity and orbital moment. As per their calculation, the NMR is temperature independent, and it increases with the movement of the Fermi energy towards the band edge.

Furthermore, the induced magnetic ordering with doping of magnetic ions in a topological insulator may create exotic topological effects in the MR by breaking the time reversal symmetry, provided the dominant charge carriers are from the topological surface states (TSS). Investigation of the role of TSS in MR in these systems is of paramount interest, however, has not been explored in details, probably due to a hindrance in the analysis and interpretation of transport data due to large carrier density of the bulk. In the literature, it has been reported that the Cr-doped $Bi_2Se_3$is paramagnetic [16]. The doped Sb_2Te_3[$Sb_{2-x}V_xTe3$, $Sb_{2-x}Cr_xTe_3$] shows a ferromagnetic (FM) order with the domination of the bulk transport of charge carriers [17,18]. Doping transition metal impurities (*i.e.*, Fe, Mn, Cr) in a TI can give rise to a well-defined FM order with perpendicular magnetic anisotropy, which provides an easiest method to open the gap of the surface state of the TI and tune the transport properties [19]. Moreover, there are controversies regarding the gap openings with the doping of the transition-metal in TI. For instance, with Fe adsorption on the surface of topological insulator the gap opening is not observed [20], whereas it is found in the Fe-doped TIs [21,22]. The most interesting observation in the Fe doped case is the decrement of the band-gap size of topological surface state (TSS) at high Fe concentrations [23]. We aim to understand how does the breaking of time reversal symmetry (*via.* long-range magnetic ordering effects) create exotic topological effects which in turn affects the MR. With this view, we present here the results of magnetic, magneto-transport and angle resolved photoemission spectroscopy (ARPES) studies forthe $Bi_{2-x}Fe_xSe_{3-x}S_x$ [with $x = 0.06$, 0.09 and 0.12; denoted as BiFeS-L, BiFeS-M and BiFeS–H respectively]. The appearance of the surface state in the present ARPES spectra and the quantum oscillation in the resistivity pattern reveal that the topological surface property is preserved with the co-doping of Fe and S. The appearance of the quantum oscillations at low field combined with the ARPES measurements clearly suggests a change in the Fermi surface with the doping. Moreover, for the BiFeS-M, we have observed a large negative MR even at room temperature, for the first time, in the transverse geometry (with electric field transverse to magnetic field). Our results suggest that the bulk ferromagnetic ordering is responsible for the observed NMR in the BiFeS-M in the transverse geometry of measurements.

2. Material and method

2.1. Synthesis

The single crystal $Bi_{2-x}Fe_xSe_{3-x}S_x$were grown by melting a stoichiometric mixture of high purity Bi, Se, Fe and S, sealed in evacuated ampoules. The ampoules were heated up to 900 °C (rate: 200 °C/h) and kept at 900 °C for 10 h and then cooled slowly to 620 °C (rate: 3 °C/h). After that it was cooled down to 550 °C (rate: 5 °C/h) and then it was naturally cooled down to room temperature. The orientation of grown crystals was checked by X-ray Laue back reflection diffraction technique.

2.2. Structural characterization

For phase confirmation, the X-ray powder diffraction (XRD) measurement were carried out using a Rigaku (mini flex II DEXTOP) Powder diffractometer with Cu K_α radiation. Fig. 1 shows the Rietveld refined x-ray diffraction patterns for BiFeS-L, BiFeS-M, and BiFeS–H using the Fullprof software. The refinement confirms the single-phase formation of these compounds in the rhombohedral structure space group (R–3m). The variation of lattice parameters with the doping concentration is shown in the inset Fig. 1 which follows the Vegard's law. The linear nature of the curve confirms that the Fe and S are successfully substituted Bi and S. The refined unit cell parameter and other structural parameters are given in Table 1. The elemental compositional analysis of all samples were obtained by energy dispersive X-ray (EDS), using Nova Nano SEM 450 (FEI, U.S.A.). The EDS graph is shown in the inset of Fig. 1.

2.3. Dc magnetization and electrical transport measurements

The electrical transport properties of all the measured samples [with dimension 5mm × 1mm × 0.16 mm(l × w × t)] were measured using a Quantum Design physical properties measurement system (9T PPMS), and the magnetic properties measurements were carried out by a superconducting quantum interference device-vibrating sample magnetometer (SQUID-VSM) of the Quantum Design make. The electrical transport and magnetic properties were also measured using a CRYOGENIC make Vibrating Sample Magnetometer (9T, VSM).

2.4. ARPES study

To probe the electronic structure of our samples, we have performed Angle Resolved photo emission Spectroscopy (ARPES) measurement. The measurement has been carried out with a μ-Laser ARPES system with photon energy of 6.3 eV at HISOR, Hiroshima University, Japan. All the measurements were done at 20K which confirmed the existence of topological surface state in the samples. All the samples were cleaved *in-situ* at 30K along the *c*-axis un an ultrahigh vacuum. A very clean mirror-like surface was seen after cleaving and found to stable more than 2 days in UHV chamber.

3. Results

3.1. Hall study

We have measured the magnetic field (H||C) variation of the Hall resistivity at different temperatures for the $Bi_{2-x}Fe_xSe_{3-x}S_x$ single crystals. In Fig. 2(a) the Hall effect data at a particular temperature (2K) has been shown. The slopes of all the curves are negative indicating that the carriers are of the *n*-type. The temperature variations of the mobility and carrier concentration have also been derived from the Hall data and particularly for BiFeS-M are plotted in the inset of Fig. 2(a). For all the samples, except for the BiFeS-L, the carrier concentration remains flat at low temperatures, and then increases with increasing the temperature. This reveals that the bulk insulating character becomes significant at higher temperature, while at low temperatures the surface metallic character dominates [12]. For all the samples, the mobility decreases with increasing the temperature, which may be due to the increased phonon scattering at high temperature. Moreover, generally ferromagnetism shows the existence of Analomous Hall effect (AHE). But, here, we did not observe any signature of AHE, which is consistent with already reported results [24–27]where the AHE is absent despite of existence of ferromagnetism. Fig. 2(b) shows the resistivity as a function of temperature for the $Bi_{2-x}Fe_xSe_{3-x}S_x$samples. The graph shows a positive slope indicating their metallic behaviour. It is observed that the resistivity value of the $Bi_{2-x}Fe_xSe_{3-x}S_x$ system first increases with increasing the doping concentration of Fe and S (undoped to BiFeS-L) and then decreases

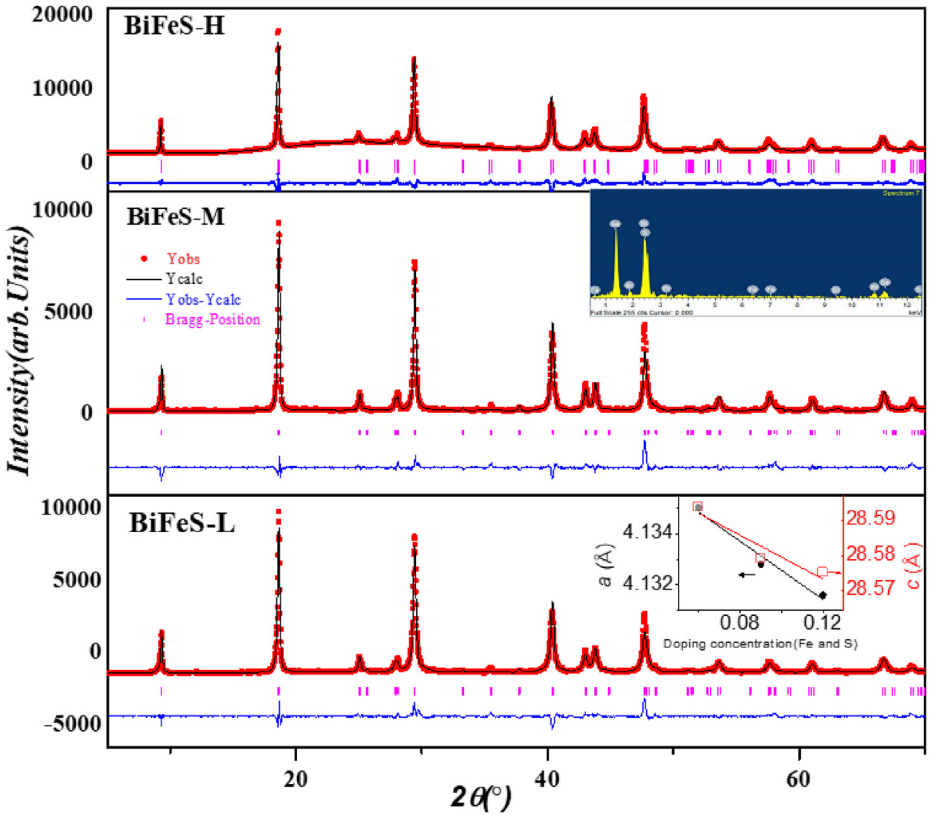

Fig. 1. Rietveld refined x-ray powder diffraction patterns at 300 K for BiFeS–H, BiFeS-M and BiFeS-L (top to and bottom). The open symbols and line represent experimental data and calculated results, respectively. The vertical bars indicate the calculated positions of nuclear Bragg reflections and the bottom line is a residual.

Table 1
Structural parameters obtained from Rietveld refinement of BiFeS-L, BiFeS-M and BiFeS-H samples.

Sample	Atom	Wyckoff position	*x*	*y*	*z*	*Occupancy*
BiFeS-L	Bi	6c	0	0	0.40281(4)	0.161667
$Bi_{1.94}Fe_{0.06}Se_{2.94}S_{0.06}$	Fe	6c	0	0	0.40281(4)	0.005
	Se1	3a	0	0	0	0.08333
	Se2	6c	0	0	0.20619(3)	0.161667
	S	6c	0	0	0.20619(3)	0.005
		$a = b = 4.135(9)$ Å, $c = 28.594(7)$ Å				
BiFeS-M	Bi	6c	0	0	0.40364(1)	0.159167
$Bi_{1.91}Fe_{0.09}Se_{2.91}S_{0.09}$	Fe	6c	0	0	0.40364(1)	0.0075
	Se1	3a	0	0	0	0.08333
	Se2	6c	0	0	0.20385(4)	0.159167
	S	6c	0	0	0.20385(4)	0.0075
		$a = b = 4.1318(7)$ Å, $c = 28.576(6)$ Å				
BiFeS–H	Bi	6c	0	0	0.40267(1)	0.156667
$Bi_{1.88}Fe_{0.12}Se_{2.88}S_{0.12}$	Fe	6c	0	0	0.40267(1)	0.01
	Se1	3a	0	0	0	0.08333
	Se2	6c	0	0	0.2049(3)	0.156667
	S	6c	0	0	0.2049(3)	0.01
		$a = b = 4.1316(7)$ Å, $c = 28.575(6)$ Å				

(BiFeS-L to BiFeS-M). When the doping concentration is increased further (BiFeS-M to BiFeS–H), the resistivity value increases. The Hall data confirm that the bulk insulating character dominates over the surface metallic character at higher temperature (Fig. 2(a)). Therefore, the lower resistivity of the BiFeS-M, as compared to the Bi_2Se_3, might be due to the bulk ferromagnetism (discussed later) in BiFeS-M. However, the crossover at low temperature is due to the surface impurity doping in BiFeS-M because at low temperature surface state dominates over the bulk state [12]. But compared to BiFeS-L the lower resistivity value throughout the whole temperature range in BiFeS-M might be due to the dominant ferromagnetic behavior.

3.2. DC-magnetization study

In order to investigate the effect of Fe doping on the magnetic ordering and hence on the magneto-transport properties we have measured the magnetization (M) as a function magnetic field (H) (H||c) (Fig. 3). A strong diamagnetic behaviour is evident for the BiFeS-L at 300 K from M(H) behavior. For the BiFeS–H single crystal,

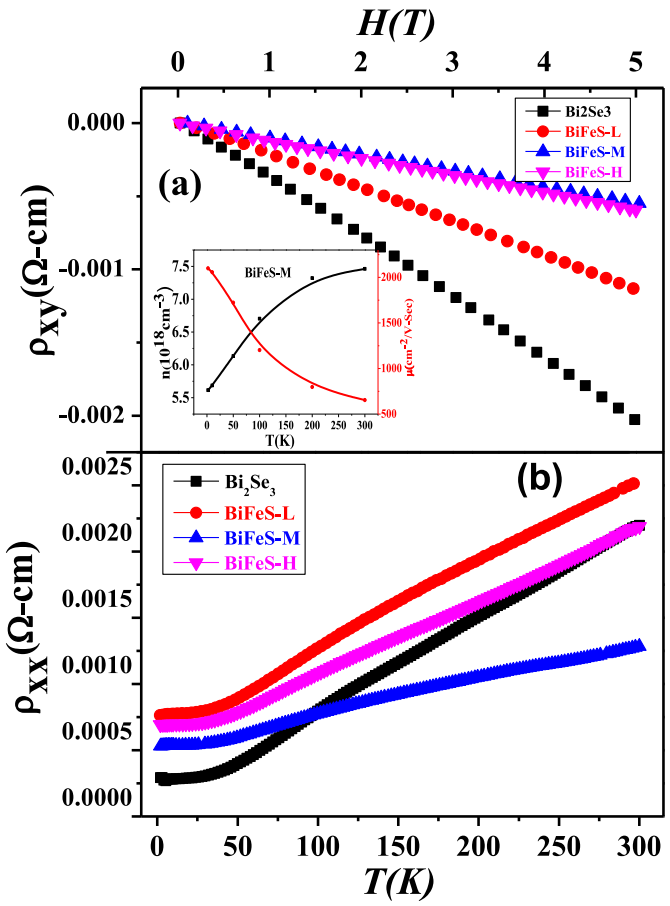

Fig. 2. (a) Hall resistivity as a function of magnetic field at 2K for Bi_2Se_3, BiFeS-L, BiFeS-M, and BiFeS−H. Insets: Temperature variation of mobility and carrier cancentration estimated from Hall data for BiFeS-M. (b) Resistivity as a function of temperature for Bi_2Se_3, BiFeS-L, BiFeS-M, and BiFeS−H.

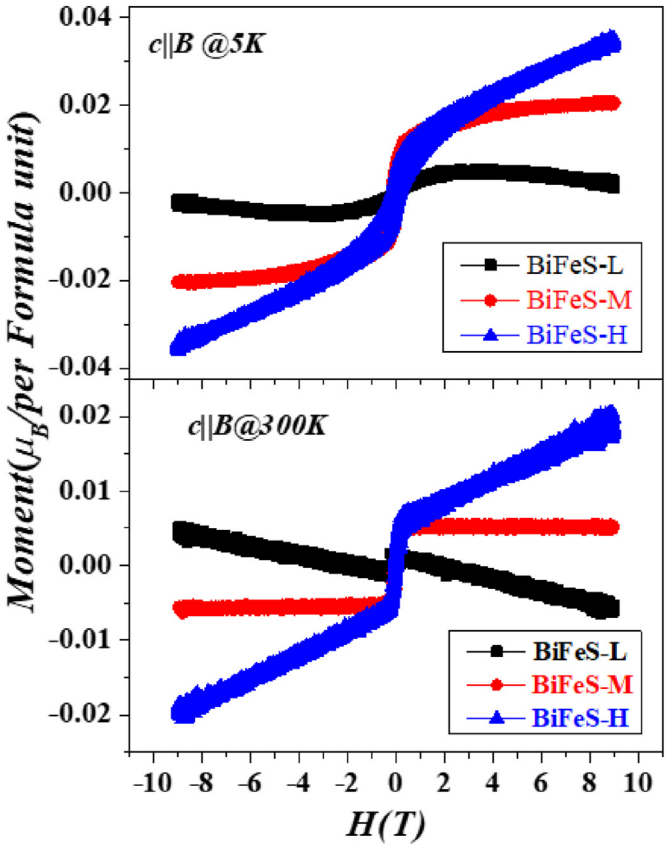

Fig. 3. Magnetization as a function of magnetic field under H = 1000 Oe for BiFeS-L, BiFeS-M, and BiFeS−H at 5K (upper panel) and 300K (lower panel).

a sharp field-induced transition to a ferromagnetic-like state is also evident at 5 K, indicating that the antiferromagnetic (AFM) ground state is fragile. The important observation in our study is that as the Fe-doping content varies magnetic ordering changes from FM (BiFeS-M) to AFM (BiFeS−H). If we assume that part of the Fe goes to surface, then the transition from FM to AFM ordering with increase of Fe concentration is consistent with the predictions of first-principles calculations [23], where it was reported that an antiferromagnetic phase mediated by the superexchange interaction was stabilized for a higher Fe-concentration. It was also reported that anti-ferromagnetically aligned neighboring Fe spins behave like nonmagnetic scattering centers preserving the time reversal symmetry. In the available reports it has been shown that the Fe doping induces magnetic ordering at low temperature [22,23]. But in the present co-doped (S and Fe) Bi_2Se_3, the magnetic ordering is observed even at 300K (for BiFeS-M). Therefore, the observed magnetic ordering might be due to the presence of both electron mediated-RKKY interaction [23] on the surface, and the bulk van Vleck mechanism. This is the reason of obtaining the FM ordering at higher temperature (room temperature) for the BiFeS-M. For the BiFeS−H sample, due to an excess doping, the formation of n-type antisite defect is promoted, which in effect forces the Fermi level E_F "pinned" far away the valence band and therefore, the van-Vleck mechanism disappears. As a matter of fact, the observed AFM in BiFeS−H is due to the surface RKKY interaction.

For FeS−H, no hysteresis indicate at AFM-like state. For FeS−H compound, an increase in the magnetization along with hysteresis loop of isothermal magnetization curves M at low temperatures confirms a FM-like state. The observed M-T curves (not shown) seemingly do not follow a usual trend as expected for an ideal FM and AFM, which could be due to a small diamagnetic contribution and/or some fraction of the magnetic impurity may open up a local gap and suppresses the local density of states. Further microscopic measurements are necessary to investigate the nature of spin-spin correlations in these compounds.

3.3. ARPES study

To investigate the topological surface states and changes in the electronic behavior of the system on Fe/S co-doping, we have carried out ARPES measurements on the $Bi_{2-x}Fe_xSe_{3-x}S_x$ samples at 20 K (Fig. 4). It is observed, for the BiFeS-L, BiFeS-M, and BiFeS−H samples, the Dirac point of the Fermi surface is located at 175 ± 2, 250 ± 3 and 225 ± 5 meV, respectively. The bright intensity is markedly suppressed for the BiFeS-M sample, suggesting that the Kramers degeneracy is lifted in BiFeS-M but the surface state still exists. Fig. 4 (b, e, h) shows the energy-distribution curve (EDCs) at $k_x = 0$. We have fitted the EDC curve using two Lorentzian function. The X-shaped surface band is split into lower and upper branches, with an energy gap of 32 ± 2, 56 ± 2, 25 ± 2 meV at the $\bar{\Gamma}$-point for BiFeS-L, BiFeS-M and BiFeS−H samples respectively. The observed gap at the Dirac point might be due to the Fe doping. Previously, some controversial results were reported about the gap opening at the Dirac point with Fe doping in Topological Insulator. In some of the reports [19], the gap opening was reported whereas in some other studies [20,29] it was claimed that no gap opening was

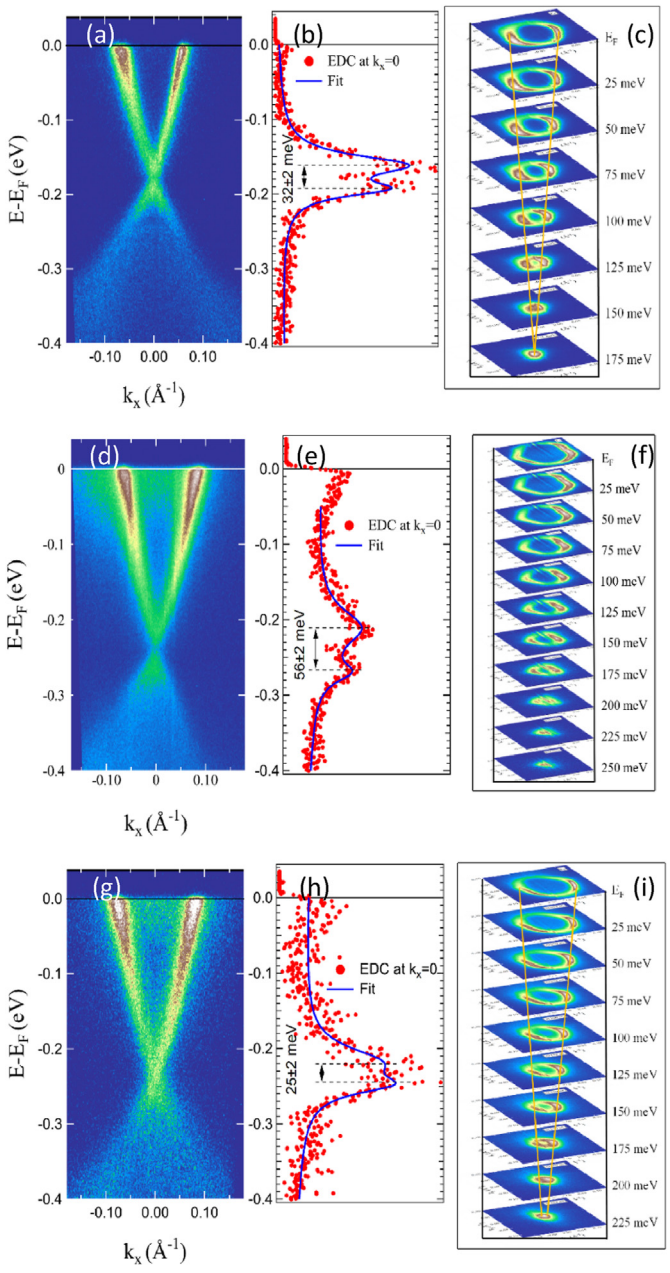

Fig. 4. ARPES of BiFeS-L, BiFeS-M, and BiFeS–H: (a, d, g) Binding energy vs. wave vector; (b, e, h): energy distribution curves; (c, f, i) constant-energy contours of the band structure show the surface states evolution from the Dirac point to the Fermi level.

observed with the magnetic ion doping. In the present investigation, both from magneto-transport (discussed below) and ARPES studies, we have observed bandgap opening at the Dirac point with the Fe-doping in the host material. However, with further increasing the doping concentration of Fe and S (BiFeS–H sample), the surface bandgap is reduced significantly. From the magnetic data it is clear that BiFeS–H is AFM in nature. Therefore, the surface gap closing is likely to correlate with the AFM ordering which is in agreement with the reported results [23]. Fig. 4 (c, f, i) shows constant-energy contours for all samples. It should be noted that all of Fe and S doped samples show hexagonally warped Fermi surfaces, which is much pronounced compared to the Fermi surface of Bi_2Se_3 [30] suggesting the modification of energy packet of conduction band at the Fermi surface. Based on the k_F values 0.05 Å^{-1}-0.08 Å^{-1} of these samples, the estimated carrier density of the topological surface state lies in the range of 2×10^{12}-5×10^{12} cm^{-2}.

3.4. Magnetoresistance study

In order to study the effect of magnetic ordering and topological surface states on the MR, we have measured out of plane ($H\perp E$) and in plane ($H||E$) magnetoresistance (MR)as a function of magnetic field at different temperatures for $Bi_{2-x}Fe_xSe_{3-x}S_x$ (shown in Fig. 5). We have defined MR as $[\{\rho(H)-\rho(0)\}/\rho(0)]*100$ %. The MR value decreases with an increase of the doping concentration. It is observed that for BiFeS-L, a quantum oscillation appears at a magnetic field ($H\perp E$) as low as ~4.5T. At low temperature, the MR value decreases with increasing magnetic field (upto ~2T), suggesting that the MR is negative. With further increasing the doping concentration **(**BiFeS-M**),** the large negative MR with the SdH oscillations are observed throughout the whole temperature and magnetic field ($H\perp E$) range of measurements as shown in Fig. 5(b). However, if the doping content is further increased (BiFeS–H), the positive MR (for $H\perp E$) reappears (Fig. 5(c)). In-plane MR ($H||E$) is shown in Fig. 5(d–f). The observed MR is strongly anisotropic for all the samples. In Fig. 5(d), it is found that the BiFeS-L sample shows a negative linear MR at low temperature (below 50K). The in-plane MR(H) behavior for the BiFeS-M is non-monotonic. Up to 10K it shows a negative MR. Initially the MR decreases with increasing magnetic field, and with further increase of magnetic field the MR increases. Above 10K, the MR becomes positive and linear. For the BiFeS–H sample, the MR(H) behaviour is similar to that for the BiFeS-L. As discussed above (ARPES), the obtained surface gap for BiFeS-L is very low but for BiFeS-M it is significantly large whereas, for BiFeS–H gap is negligibly small. Therefore, the surface gap plays a significant role in the behaviour of MR.

For the $H\perp E$ configuration, the quantum oscillations appear for all three samples, suggesting that the quantum oscillations appear for the surface states. However, for BiFeSe-L, we observe a quantum oscillation at the lowest temperature of measurement even for $H||E$, suggesting that the quantum oscillations appear both for bulk and surface states [31]. The variation of the amplitude of the quantum oscillation with the inverse magnetic field for the $H\perp E$ configuration is shown in Fig. 6(a-c). The amplitude of oscillation decreases with increase of temperature. Moreover, the oscillation amplitude gradually decreases with the doping content, suggesting the presence of doping induced additional defects that contribute to the charge-carrier scattering. To analyze the oscillations, we have carried out the fast Fourier transform as shown in the inset of Fig. 6(a-c). It is observed from the inset of Fig. 6(a-c) that there exists a single frequency for all the doped samples which is in sharp contrast to the undoped sample [14] where three frequencies are found. The existence of single frequency suggests that there might be a single packet (for the surface states) at the Fermi surface which agrees with the ARPES data where it is observed that with doping a hexagonal warping appears in the Fermi surface (Fig. 4). The amplitude of frequency decreases with increasing the temperature, but the frequencies remain same at all the temperatures. Furthermore, the oscillation depends only on normal component of H which suggests that the Fermi surface is of two-dimensional. The observed small oscillation in the in-plane MR for the BiFeSe-L could be due to the hexagonal warping of the Fermi surface. With the help of the Onsager's relation the calculated relative Fermi wave vector k_F, are 4.36×10^8, 4.56×10^8 and 3.87×10^8 m^{-1},respectively for BiFeS-L, BiFeS-M, and BiFeS–H samples. These values are consistent with the values calculated from the ARPES results. Moreover, the obtained effective mass m^* from the SdH oscillation

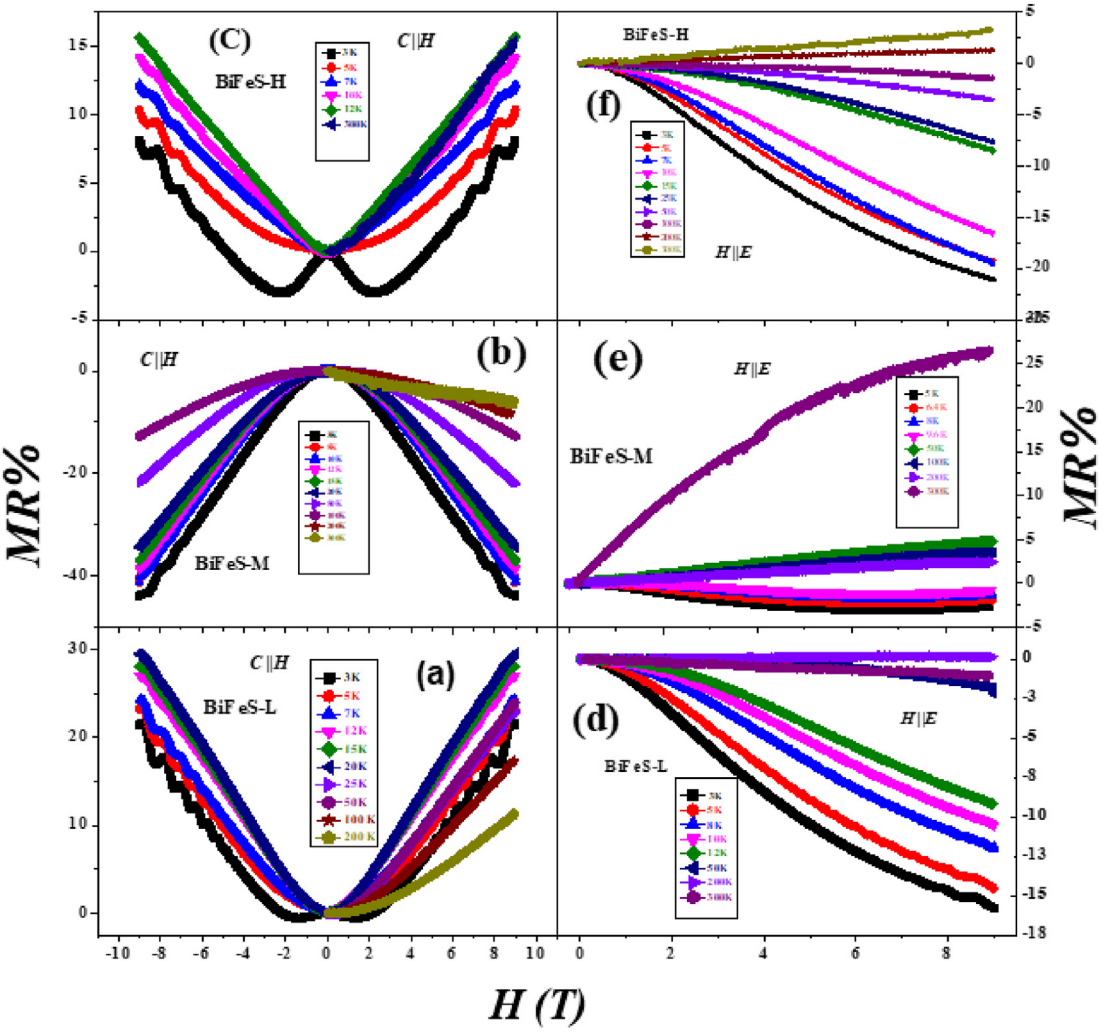

Fig. 5. MR as a function of magnetic field at different temperatures for BiFeS-L, BiFeS-M, and BiFeS–H for out-of-plane magnetic field (a–c); for in-plane magnetic field (d–f).

amplitude [32]found to be 0.17, 0.18 and 0.12 m_e, respectively for BiFeS-L, BiFeS-M and BiFeS–H indicating that inthe FM state the Dirac Fermion becomes massive. Using the linear dispersion relation for the surface state $V_F = \hbar k_F/m^*$, the estimated Fermi velocities of BiFeS-L, BiFeS-M and BiFeS–H are 2.97×10^5, 3.52×10^5 and 4.07×10^5 m/s respectively. These values are consistent with the Dirac surface state, and the largest value for BiFeS–H suggests the presence of a robust surface state with the narrow Dirac cone. The above discussion clearly suggests that the quantum limit is reached in the present case at very low magnetic field (~4.5T).

Furthermore, it is clear from the magnetization measurement that, BiFeS-Mshows a ferromagnetic ordering throughout the whole temperature range of measurement (2–300K), which might be responsible forthe NMR in the BiFeS-M. For the compounds BiFeS-L and BiFeS–H, we observe a positive MR in the perpendicular magnetic field configuration, and a negative MR (NMR) in the *H||E* configuration. A NMR has also been reported in low-dimensional (1D and 2D) charge ordered systems for *H||E* configuration [33,34]. However, the observation of a large MR (either positive or negative) cannot be explained with the classical theory as it suggests the vanishing MR, due to the absence of Lorentz force for *H||E* configuration [31], and the experiments also suggest the presence of a quantum-mechanical effect. It is also worthwhile to mention that the negative longitudinal magnetoresistance (LMR) for BiFeS-L and BiFeS–H is not due to the field induced suppression of the scattering from the ferromagnetic spins as same is not observed for the transverse MR in the present investigation. Furthermore, a classical origin, attributed to the macroscopic inhomogeneities [36], can be excluded as this cannot be the case in the present investigation [see Ref. 12 for sample characterization]. However, a negative LMR was predicted by Argyres and Adam in non-degenerate semiconductors with the presence of an ionized impurity scattering [37]. There are reports that $Bi_{1-x}Sb_x$ and $ZrTe_5$ show a large negative LMR [38,39]. On the other hand, when *E* and *H* are perpendicular, these materials show positive transverse magnetoresistance (TMR) similar to the present investigation. The sharp negative LMR [38,39] at low field is associated with the WAL which arises from the strong spin-orbit coupling in these materials [40]. In the present case the TMR data showed weak antilocalization (WAL). On the other hand, in the longitudinal MR existence of WAL is not observed indicating the weak antilocalization is due to 2D Dirac fermions. The negative longitudinal magnetoresistance (positive magneto-conductivity (MC)) at low magnetic field can be described by the semiclassical theory by considering the Berry curvature [5]. In this case the most important observation is the variation of longitudinal MC as H^2, which originates due to the topological E.H term. This E.H term has an additional contribution to the momentum along perpendicular to the plane, driven by the

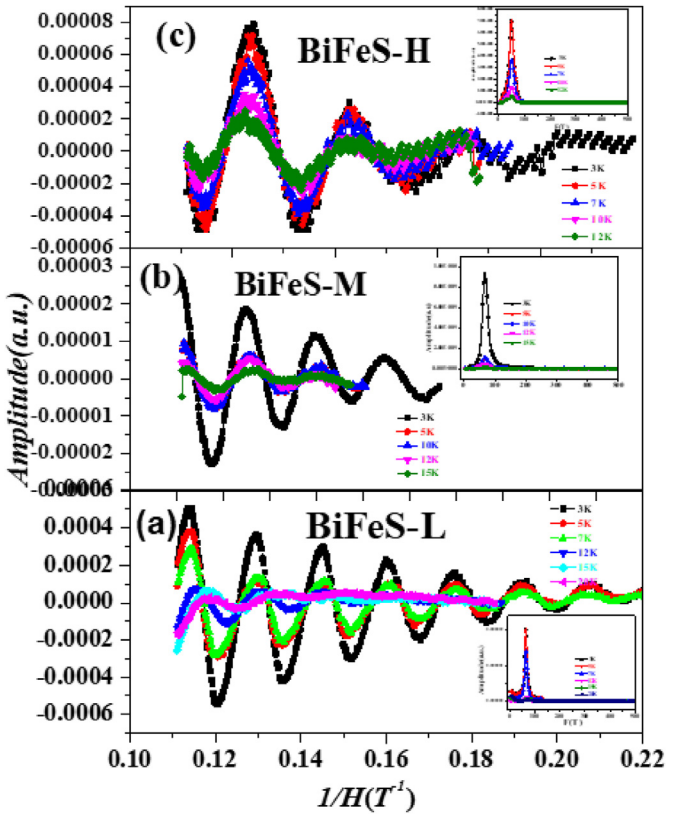

Fig. 6. (a-c)The variation of the amplitude of the quantum oscillation with the inverse magnetic field for the $H \perp E$ configuration. Insets: First Fourier Transform of SdH oscillations of data shown for BiFeS-L, BiFeS-M, and BiFeS–H.

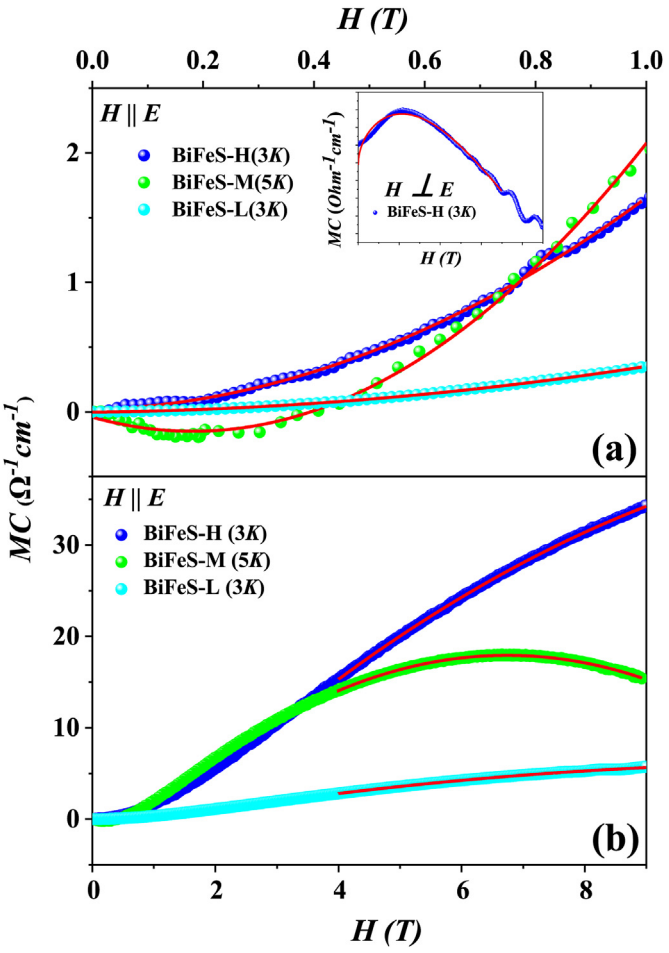

Fig. 7. For H||Econfiguration Longitudinal Magneto Conductivity (MC) (a) fitted as a function of H2 up to 1T, (b) LMC dependency on both H and H2 above 4T forBiFeS-L,BiFeS-M, and BiFeS–H. Inset: Transverse Magneto Conductivity fitted as $\sigma_T(H) = 1/\rho_{wal} + 1/\rho_n$for BiFeS–H at 3K for H⊥Econfiguration. For all the cases solid red line is the fitted curve.

in plane parallel electric and magnetic fields under the influence of Berry curvature. The momentum transfer causes the enhancement of the longitudinal conductivity proportional to the applied magnetic field. On the other hand, the transverse MC (in absence of E.H) is expressed as $\sigma_T(H) = 1/\rho_{wal} + 1/\rho_n$ where $\rho_n = \rho_0 + AH^2$ (with ρ_0 and A are constants)[Fig. 7]. WAL and normal contributions have been added as they originate from different bands [5]. We have seen that in our case upto 2T magnetic field the LMC varies as H^2. Above 2T the fitting is not well[Fig. 7(a)]. Therefore, upto 2T the MR behaviour can be explained with the semiclassical theory.

4. Discussion

Recently it has been proposed that in topological materials, the axial anomaly, a quantum mechanical phenomenon can give rise to a longitudinal NMR [41–44]. However, the axial anomaly can also give rise to a very large longitudinal NMR for certain gapless semiconductors [45], where conduction and valence bands linearly intersect each other at the Brillouin zone. Under the application of a magnetic field, the charge carriers are quantized into the Landau levels with a 1D dispersion along the magnetic field direction and in addition to this for $H||E$ configuration, a uniform acceleration of the center of mass in this field-induced 1D system produces the axial anomaly effect. This reduced dimensionality of the electronic dispersion has also been proposed as the origin of the observed NMR in the interplanar resistivity of 2D correlated metals [46]. In the present investigation the estimated quantum limit is at a field strength ~10T for all the samples with the carrier concentration of ~10^{18} cm^{-3} [Fig. 1]. However, from the MR data it is observed that the quantum limit is reached ~4.5 T as quantum oscillations appear at this field only. It is observed [Fig. 7(b)] that in the longitudinal configuration above 5T LMC can be expressed as function of both H^2 and H ($\sigma(H) = A_1H + A_2H2$). The H^2 dependency is due to the long-range ionic impurity scattering which gives rise to a large positive LMC in the quantum limit. On the other hand, H dependency is due to the short-range neutral impurity scattering. This indicates that the generic axial anomaly induced LMC and LMR in the quantum limit is due to the presence of short-range neutral impurities and long-range ionic impurities [44]. Because of the neutral short-range impurities, the slope in the LMC decreases which is dependent on the underlying band structure. Therefore, the axial anomaly is the driving mechanism behind the observed negative LMR in the present BiFeS-L and BiFeS–H samples in the quantum limit. Further, the MR for BiFeS-M for in-plane magnetic field is quite different than those of BiFeS-L and BiFeS–H. This might be due to the combined effect of ferromagnetic ordering and axial anomaly. In BiFeS-M the MR passes through a minimum which further support the existence of axial anomaly. In this material the FM ordering suppresses the H2 dependency (long range ionic scattering) and in effect of which the impurity scattering dominates. Therefore, in the quantum limit, in the presence of FM ordering, the combined effects of neutral and ionic impurities initially lead to a negative LMR,

which ultimately becomes positive after passing through a minimum. Furthermore, for $H \perp E$ configuration interestingly it is observed that for BiFeS-L and BiFeS–H samples at lowest temperature the MR is minimum and with increase of temperature it increases up to 50K and then start decreasing. It is observed that above 50K quantum oscillation disappears indicating that system is no more in the quantum limit. Therefore, the axial anomaly effect does not exist above 50K and normal MR behaviour is observed.

5. Conclusion

The magnetic, magneto-transport and ARPES studies have been carried out for the $Bi_{2-x}Fe_xSe_{3-x}S_x$Topological insulators. The magnetic ordering induced by Fe and S co-doping can be explained by the RKKY interaction. For $x = 9$ % (BiFeS-M), a FM is induced and the surface band gap is opened at Dirac point. With further doping (for $x = 12$ %, BiFeS–H), magnetic ordering changes to AFM and the surface band gap is suppressed as compared to BiFeS-L and BiFeS-M. The low doped ($x = 6$ %) and high doped (x = 12 %) samples show a positive MR for $H \perp E$ and a NMR for $H \| E$ whereas the $x = 9$ % doped sample shows NMR for both the field configurations. The NMR behaviour of the $x = 9$ % sample has been attributed to the strong FM ordering whereas, the MR behaviour for the $x = 6$ % and $x = 12$ % at lower magnetic field have been explained with the semi classical theory whereas at higher field the MR have been attributed to the axial anomaly. The BiFeS–H appears to be a promising candidate for antiferromagnetic topological insulators with non-trivial topological surface states. The appearance of Shubnikov-de Haas oscillations (SdH) in resistivity pattern reveals that the topological surface state is preserved with the co-doping of Fe and S. The results presented in this work would draw the attention of scientific community to investigate the magnetroseistance of other magnetically doped topological insulators.

Declaration of competing interest

The authors declare that they have no known competing financial interests or personal relationships that could have appeared to influence the work reported in this paper.

Acknowledgement

Authors are grateful to CIF, IIT(BHU) for providing magnetic measurement facility. The ARPES measurements were performed with the approval of the Proposal Assessing Committee of the Hiroshima Synchrotron Radiation Center (Proposal Numbers: 18AG029 and 18BG031).

References

[1] Breunig O, Wang Z, Taskin AA, Lux J, Rosch A, Ando Yoichi. Nat Commun 2017;8:15545. https://doi.org/10.1038/ncomms15545.
[2] Dai X, Du ZZ, Lu H. PhysRev Lett 2017;119:166601.
[3] Xiong J, Kushwaha SK, Liang T, Krizan JW, Hirschberger M, Wang W, Cava RJ, P N. Nature 2015;350:413–6.
[4] Son DT, Spivak BZ. Phys Rev 2013;B88:104412.
[5] Kim HJ, Kim KS, Wang JF, Sasaki M, Satoh N, Ohnishi A, Kitaura M, Yang M, Li L. Phys Rev Lett 2013;111:246603.
[6] Arnold F, Shekhar C, Shu-ShunWu, Sun Y, Resis R, Kumar N, Naumann M, Ajeesh M, et al. Nat Commun 2016;7:11615. https://doi.org/10.1038/ncomms11615.
[7] Li H, He HT, Lu HZ, Zhang HC, Liu HC, Ma R, Fan ZY, Shen SQ, Wang JN. Nat Commun 2016;7:10301.
[8] Li CZ, Wang LX, Liu HW, Wang J, Liao ZM, Yu DP. Giant. Nat Commun 2015;6:10137.
[9] Wiedmann S, Jost A, Fauque B, van Dijk J, Meijer MJ, Khouri T, Pezzini S, Grauer S, Schreyeck S, Brune C, Buhmann H, Molenkamp LW, Hussey NE. Phys Rev B 2016;94. 081302(R).
[10] He HT, Liu HC, Li BK, Guo X, Xu ZJ, Xie MH, Wang JN. Phys Lett 2013;103:031606.
[11] Wang L-X, Yan Y, Zhang L, Liao Z-M, Wu H-C, Yu D-P. Zeeman, nanoribbons. Nanoscale 2015;7:16687.
[12] Singh R, Shukla KK, Kumar A, Okram GS, Singh D, Ganeshan V, Lakhani A, Ghosh AK, Chatterjee S. J Phys: Condens Matter 2016;28:376001.
[13] Breunig O, Wang Z, Taskin AA, Lux J, Rosch A, Ando Y. Nature communation 2017:15545.
[14] Goswami P, Pixley JH, Das Sarma S. Phys Rev B 2015;92:075205.
[15] Dai Xin, Du ZZ, Lu Hai-Zhou. Phys Rev Lett 2017;119:166601.
[16] Liu M, Zhang J, Chang C-Z, Zhang Z, Feng X, Li K, He K, Wang L-L, Chen X, Dai X, Fang Z, Xue Q-K, Ma X, Wang Y. Phys Rev Lett 2012;108:036805.
[17] Zhou Z, Chien Y-J, Uher C. Phys Rev 2006;B74:224418.
[18] Dyck JS, Hájek P, Lošťák P, Uher C. Phys Rev 2002;B65:115212.
[19] Qi XL, Zhang SC. Rev Mod Phys 2011;83:1057.
[20] Scholz MR, Sánchez-Barriga J, Marchenko D, Varykhalov A, Volykhov A, Yashina LV, Rader O. Phys Rev Lett 2012;108:256810.
[21] Chen YL, Chu J-H, Analytis JG, Liu ZK, Igarashi K, Kuo H-H, Qi XL, MoR SK, Moor G, Lu DH, Hashimoto M, Sasagawa T, Zhang SC, Fisher IR, Hussain Z, Shen ZX. Science 2010;329:659.
[22] Kim Heon-Jung, Kim Ki-Seok, Wang J-F, Kulbachinskii VA, Ogawa K, Sasaki M, Ohnishi A, Kitaura M, Wu Y-Y, Li L, Yamamoto I, Azuma J, Kamada M, Dobrosavljević V. Phys Rev Lett 2013;110:136601.
[23] Kim J, Jhi S. Phys Rev B 2015;92:104405.
[24] Zhang D, Richardella A, Rench DW, Xu SY, Kandala A, Flanagan TC, Beidenkopf H, Yeats AL, Buckley BB, Klimov PV, Awschalom DD, Yazdani A, Schiffer P, Hasan MZ, Samarth N. Phys Rev B 2012;86:205127.
[25] Liu N, Teng J, Li Y. Nat Commun 2018;9:1.
[26] Kilanski L, Dobrowolski W, Dynowska E, Wjcik M, Kowalski BJ, Nedelko N, Lawska-Waniewska A, Maude DK, Varnavskiy SA, Fedorchenko IV, Marenkin SF. Solid State Commun 2011;151:870.
[27] Maryenko D, Mishchenko AS, Bahramy MS, Ernst A, Falson J, Kozuka Y, Tsukazaki A, Nagaosa N, Kawasaki M. Nat Commun 2017;8:1.
[29] Valla T, Pan Z-H, Gardner D, Lee YS, Chu S. Phys Rev Lett 2012;108:117601.
[30] Kuroda K, Arita M, Miyamoto K, Ye M, Jiang J, Kimura A, Krasovskii EE, Chulkov EV, Iwasawa H, Okuda T, Shimada K, Ueda Y, Namatame H, Taniguchi M. Phys Rev Lett 2010;105:076802.
[31] Wang X, Du Y, Dou S, Zhang C. Phys Rev Lett 2012;108:266806.
[32] Shoenberg D. Magnetic oscillations in metals. Cambridge, England: Cambridge University; 1984.
[33] Xu Xiaofeng, Bangura AF, Analytis JG, Fletcher JD, French MMJ, Shannon N, He J, Zhang S, Mandrus D, Jin R, Hussey NE. Phys Rev Lett 2009;102:206602.
[34] Graf D, Brooks JS, Choi ES, Uji S, Dias JC, Almeida M, Matos M. Phys Rev B 2004;69:125113.
[36] Hu Jingshi, Parish Meera M, Rosenbaum TF. Phys Rev B 2007;75:214203.
[37] Argyres PN, Adams EN. Phys Rev 1956;104:900.
[38] Kim Heon-Jung, Kim Ki-Seok, Wang J-F, Sasaki M, Satoh N, Ohnishi A, Kitaura M, Yang M, Li L. Phys Rev Lett 2013;111:246603.
[39] Qiang Li, Dmitri E. Kharzeev, Cheng Zhang, Yuan Huang, I. Pletikosic, A. V. Fedorov, R. D. Zhong, J. A. Schneeloch, G. D. Gu, T. Valla, arXiv: 1412.6543.https://arxiv.org/ct?url=https%3A%2F%2Fdx.doi.org%2F10.1038%2Fnphys3648&v=defdf745.
[40] ShinobuHikami, Larkin Anatoly I, Nagaoka Yosuke. Prog Theor Phys 1980;63:707.
[41] Arnold Frank, Chandra Shekhar, Wu Shu-Chun, Sun Yan, dos Reis RD, Kumar Nitesh, Naumann Marcel, Ajeesh Mukkattu O, Schmidt Marcus, Grushin Adolfo G, Bardarson Jens H, Baenitz Michael, Sokolov Dmitry, Borrmann Horst, Nicklas Michael, Felser Claudia, Hassinger Elena, Yan Binghai. Nat Commun 2016;7:11615.
[42] Novak Mario, Sasaki Satoshi, KoujiSegawa, Ando Yoichi. Phys Rev B 2015;91.041203(R).
[43] Xiong Jun, Kushwaha Satya, Krizan Jason, Tian Liang, Cava RJ, Ong NP. Europhys Lett 2016;114:27002. https://doi.org/10.1209/0295-5075/114/27002.
[44] Goswami Pallab, Pixley JH, Das Sarma S. Phys Rev B 2015;92:075205.
[45] Nielsen HB, MasaoNinomiya. Phys Lett B 1983;130:389. https://doi.org/10.1016/0370-2693(83)91529-0.
[46] Kikugawa N, Goswami P, Kiswandhi A, Choi ES, Graf D, Baumbach RE, Brooks JS, Sugii K, Iida Y, Nishio M, Uji S, Terashima T, Rourke PMC, Hussey NE, Takatsuw H, Yonezawa S, Maenoand Y, Balicas L. Nat Commun 2016;7:10903. https://doi.org/10.1038/ncomms10903.

Rahul K. Singh, Rahul Singh currently completed his Post-doctoral programme from Bhabha Atomic Research Centre (BARC),Mumabi, India in field of Dirac semimetal. He got his M.Tech degree in Department of Ceramic Engineering in 2013 from Indian Institute of technology Banaras Hindu University (IIT BHU), India. After that he received Ph.D. degree from Indian Institute of technology Banaras Hindu University, India. During, his research, he worked on Multiferroic materials and topological Insulator and handle the growth of single crystal along with studies of transport and magnetic properties.

S. M. Yusuf, Dr. S M Yusuf is currently the Associate Director, Physics Group of Bhabha Atomic Research Centre, Mumbai, India, and Director, Institute of Physics, Bhubaneswar. He is also a Senior Professor in Homi Bhabha National Institute, Mumbai. He completed his Ph D from University of Mumbai in 1997. He was a post-doctoral fellow at Argonne National Laboratory, USA, and a visiting scientist at the Institute of Materials Science, Spain. He has expertise in the area of magnetism and neutron scattering. In particular, he has worked extensively on low dimensional magnetism, quantum magnetism, the phenomena of magnetization reversal and magnetic proximity effects, molecular magnetism, high magnetocaloric effect, CMR perovskites, *etc.* His H-index is 45 as per the google scholar. Dr. S M Yusuf is a fellow of the Indian Academy of Sciences, National Academy of Sciences, India, and the Maharashtra Academy of Sciences, India. Presently, he serves as (i) Vice Chair, Division of Condensed Matter Physics, Association of Asia Pacific Physical Society, (ii) Board member of The Asia-Oceania Neutron Scattering Association (iii) Vice-President, Materials Research Society of India, (iv) President, Neutron Scattering Society of India, (v) INSA nominated member of the National Committee for International Union of Crystallography (IUCr), (2020–2023). He also served as (i) Vice- President of Indian Physics Association (2018–2020), and (ii) Vice President, Indian Crystallographic Association (2016–2019).

Sandip Chatterjee, Sandip Chatterjee is a Professor in the Department of Physics, Indian Institute of Technology Varanasi (BHU). He received his Ph.D. degree from IACS, Kolkata in 1997. Prior to joining the faculty of IIT (BHU), He had served as visiting fellow in Department of CMP and MS, TIFR, Mumbai. He was post-doctoral fellow at Department of Physics, National Sun Yat Sen University, Taiwan. His research interest focuses on the Topological Insulator, High T_c Superconductors and Colossal Magneto-resistive materials, Heavy Fermion System, Critical Behavior, and Strong Electron Co-relations in Solids.